Available online at www.sciencedirect.com
SCIENCE DIRECT®

Journal of the European Ceramic Society 24 (2004) 3399–3408

www.elsevier.com/locate/jeurceramsoc

Preparation of interpenetrating ceramic–metal composites

A. Mattern[a,*], B. Huchler[b], D. Staudenecker[b], R. Oberacker[a], A. Nagel[b], M.J. Hoffmann[a]

[a]*Universität Karlsruhe, Institut für Keramik im Maschinenbau—Zentrallaboratorium, Haid-und-Neu-Str. 7, D-76131 Karlsruhe, Germany*
[b]*Fachhochschule Aalen, Fachbereich Werkstofftechnik, Beethovenstr. 1, D-73430 Aalen, Germany*

Abstract

Ceramic reinforced metals are attractive because of their enhanced elastic modulus, high strength, tribological properties and low thermal expansion. Most work in this sector has focused on particle- or fiber-reinforced composites where the ceramic phase is not continuous. This work presents aluminium–alumina composites where both phases are interpenetrating throughout the microstructure. Ceramic preforms were produced with sacrificial pore forming agents leading to porosities between 50% and 67%. Pore wall microstructure was varied by changing the sintering temperature. Permeability and strength was measured for the porous preforms and infiltration results were compared with theoretical predictions based on capillary law and Darcian flow. A direct squeeze-casting process was used to infiltrate the preforms with aluminium resulting in an interpenetrating microstructure on both macropore and micropore scale.

Keywords: $A1_2O_3$; Metal matrix; Microstructure-final; Porosity; Slip casting

1. Introduction

Metal matrix composites (MMCs) have been under investigation for more than 30 years with some successful commercial applications emerging with enhanced material properties and reduction in processing costs summarised e.g. by Lloyd[1] and Clyne.[2,3] Inclusions of a ceramic phase are used in light metals like aluminium and magnesium to achieve higher strength, stiffness, hardness, wear resistance and reduced coefficient of thermal expansion. The main drawback of the material has been the high costs associated with the processing and the loss of ductility of the material.

It is interesting to see the subject matters from both sides, as the closely related ceramic matrix composites (CMCs) incorporate metal phases to increase toughness of the brittle ceramic matrix that also have been investigated[4,5] thoroughly. Traditionally, the continuous phase of the composite has been designated as the matrix. More recently, interest has arosen in composites where both phases are continuous, resulting in an interpenetrating microstructure.[6, 7] One method to achieve such a microstructure is the infiltration of a molten metal into a porous ceramic body called a preform.

The research reported here is part of an ongoing, interdisciplinary project to get an understanding of the influence of the preform microstructure and its properties on the properties of the resulting composite. With this knowledge preforms can be fabricated that fulfill the individual requirements of potential applications. Previous research suggests that there is a large potential to improve composite properties with tailored interpenetrating microstructures. Both theoretical models and experimental data indicate an increase in Young's modulus with an increase of continuity of the reinforcing phase.[8] One of the main drawbacks of MMCs is the loss of ductility compared to the matrix metal which can be alleviated with tailored microstructures: Nardone reports[9] an order of maginitude increase in notched Charpy impact energy adsorption and a strong increase in failure strain by incorporating pure metal ligaments of approximately 200 μm thickness between several MMC reinforced regions of 2 mm diameter each. For brittle ceramic microstructures reinforced with metal ligaments theoretical and experimental research[7,10–12] indicate an increase of fracture toughness with increasing ligament diameter. Sacrificial pore forming agents that are burned off before sintering as presented in this article offer an easy way to influence the pore size and shape distributions. Thus the influence of the ceramic microstructure on the composite properties can be investigated for a broad and varied range of materials.

* Corresponding author.
E-mail address: andreas.mattern@ikm.uni-karlsruhe.de (A. Mattern).

0955-2219/$ - see front matter © 2003 Elsevier Ltd. All rights reserved.
doi:10.1016/j.jeurceramsoc.2003.10.030

One of the main factors holding back more widespread commercial adoption of MMCs are the associated processing costs. Because of this, the work presented here focuses on the infiltration of preforms using squeeze casting, a standard metallurgical casting processes. One of the goals is to find preforms that can be integrated into standard commercial metallurgical processes with a minimum of changes to them.

2. Theoretical background

2.1. Processing of interpenetrating microstructures

Metal matrix composites is a large field of strong interest because of the immense potential. Most research and emerging commercial applications have focused on particle and fiber reinforcements.[1–3] Nevertheless, several interesting processing routes have been examined to achieve fully interpenetrating networks.[6] The basic step in all non-reactive methods is to produce a ceramic body which has a network of continuous open porosity. This ceramic preform is then infiltrated with a metal melt. Due to the non-wetting nature of most metal melts, especially the technologically interesting aluminium, this requires an external pressure to fill the pores which will be discussed below.

2.1.1. Sintering of coarse powders

The easiest and most commonly used way to achieve a porous ceramic preform is the sintering of coarse ceramic powders or the incomplete densification of finer powders. This technique allows influencing of the total porosity to some extent by changing the powder compaction and sintering temperature, though it is very difficult to achieve porosities above 50%. It is possible to alter the metal ligament diameter to some small extent by changing the size of the particles[7,13,14] though the particle size itself sets an upper limit to that. With this technique it is not possible to influence the pore structure independent of the ceramic microstructure.

2.1.2. Foam based methods

Another interesting approach to produce fully interpenetrating networks at low porosities has been suggested by Lange et al.[15] who slip-cast a ceramic suspension into a reticulated polymeric foam. After drying, burnout of the polymer and sintering this leaves a negative replica of the foam with fully open porosity which was then infiltrated with molten aluminium. By varying the polymeric foam a variety of ligament diameters could be achieved, though not independent of the foam 's cell size and the total porosity and hence metal volume fraction of this method was limited to about 10%.

A related technique has been reported by Cichocki et al.[16] that compressed thermoplastic polymer foams and fixed the compressed state by heating to 200 °C with subsequent cooling. By cutting the foams into, e.g. wedge shapes prior to compression to a uniform thickness, porosity gradients could be achieved. Subsequent slip casting, burnout and sintering as above lead to interpenetrating, functionally graded networks with open porosity that have been successfully infiltrated with aluminium melts. Preform porositities between approximately 5% and 25% were possible with this method.

Another foam-based approach has been reported by Peng et al.[17] who used a direct foaming and reticulation technique on suspensions of coarse alumina powder and short Saffil alumina fibers. This lead to an open-celled ceramic foam of approximately 94% porosity which was then infiltrated with molten aluminium in a squeeze-casting process.

2.1.3. Pore forming agents

The usage of sacrificial pore forming agents is a very flexible method to achieve porous ceramic parts. With this method pyrolysable particles are added to the ceramic powder during processing. During a burn-off step in processing before sintering the particles are pyrolysed, leaving pores of corresponding shape and size in the matrix. A large variety of pore forming agents (PFAs) has been reported in previous works, among them carbon fibers[15] and flakes,[18–20] wax,[20] starch,[21–23] suspension PVC[24] and polyethylene.[21] The method is very flexible as the total porosity can be controlled in the range of 0 to approximately 75% by the amount of added PFA. By default, the porosity created is not open, especially at low PFA additions. Percolation thresholds are in the range of 15–30%, depending on PFA size, shape and homogenity of distribution leading to an interpenetrating network. The green compact consolidation can be either dry-pressing or suspension-based processes which allow a further influence on microstructure. Alignment of non-spherical particles in a suspension flow is possible, as well as the creation of functional porosity gradients by using a special pressure filtration technique.[25,26]

2.2. Aluminium infiltration

Due to the non-wetting nature of most metal melts on ceramic substrates, no spontaneous infiltration of the metal into the preform is possible without reactive systems under carefully controlled conditions, such as the PRIMEX process and related efforts.[27,28] To overcome this problem, the metal melt has to be infiltrated by applying an external pressure. Garcia-Cordovilla has published an excellent review on pressure infiltration of liquid metals into packed ceramic particulates.[29] The most often used methods for infiltration are by gas pressure applied onto the melt surface[13,29,30] and direct.

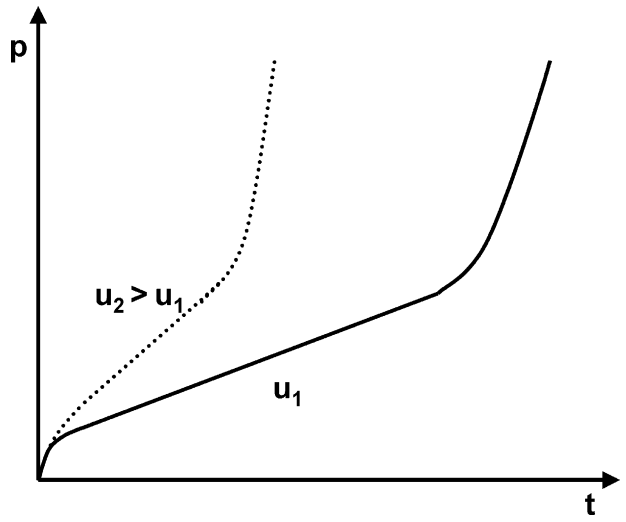

Fig. 1. Overview of the pressure increase during squeeze casting for two melt velocities.

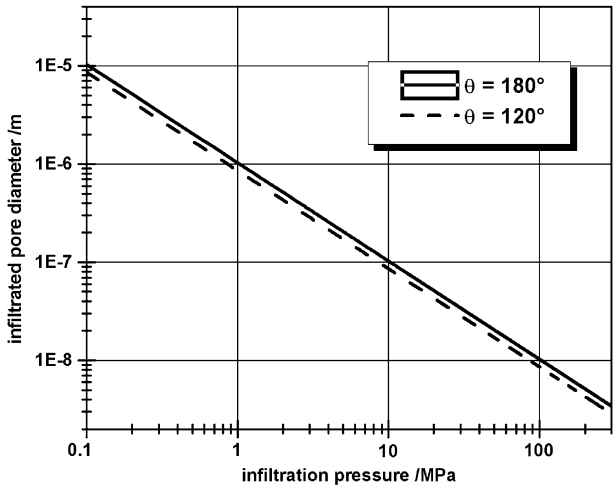

Fig. 2. Infiltrated pore diameter depending on pressure.

squeeze casting.[15,31] Of great interest is the infiltration on commercial die casting equipment, but so far only very few studies have been reported on this technique using fiber reinforcements.[32,33]

Fig. 1 shows a schematic overview of the pressure dependent on infiltration time for a squeeze-casting process. Two different infiltration velocities u_1 and u_2 are plotted with a_2 being higher than u_1. Three phases are visible: Infiltration initiation until the capillary threshold pressure is reached, stable melt flow during which the pressure increases linearly with increasing infiltration height, and compression with filling of micropores after the penetrating-through pressure has been reached and the melt front in the macropores has penetrated the whole sample. The phases will be discussed in detail below.

2.2.1. Infiltration initiation

Before the metal melt infiltrates the preform, a threshold pressure has to be overcome as the aluminium/alunmimia system is non-wetting with contact angles greater than 90°. This pressure P_0 can be calculated using capillary law as

$$P_0 = \frac{\sigma_{\text{surface}}}{r_{\text{hydraulic}}}\cos\theta \quad (1)$$

with the melt surface tension σ_{surface}, the hydraulic radius $r_{\text{hydraulic}}$ and the contact angle θ. Assuming cylindrical pores in the preform, the pore diameter that can be penetrated by a given external pressure can be calculated with the above equation as shown in Fig. 2. Surface tension for pure aluminium and air has been reported between 850 mJ/m^2 and 1100 mJ/m^2.[34] The lower values were from measurements on untreated samples whereas the higher values were for ion-cleaned surfaces. A value of 860 mJ/m^2 has been used for the calculations in this work. For the contact angle of aluminium on alumina a wide range of experimental data has been reported, with values given between 80° and 170° in vacuum.[35] This uncertainty is due to the oxide film surrounding liquid aluminium even under vacuum conditions for temperatures under 1000 °C. It has been shown that the contact angle strongly depends on the oxide film thickness. Values of 180 amid 120° have been used for the above calculations; 180° represents the worst case with a completely non-wetting behaviour which leads to the highest pressures needed to infiltrate a given pore or for a fixed pressure the smallest diameter that can be infiltrated. Given the range of pore sizes typically present in a porous ceramic, the effect of the contact angle is minor. It is important to note that the compressive strength of the preform has to be higher than the threshold pressure. Otherwise a deformation or cracking of the preform will occur. As shown in Fig. 2, a threshold pressure in the order of 1 MPa is expected for pore channels in the order of several μm diameter. This corresponds well with experimental observations on threshold pressures.[29,30] No preform deformations are expected for the materials used in this work, though pressures in this range pose a problem for fiber arrangements.

2.2.2. Melt flow

Once the threshold pressure has been overcome, the molten metal flows into the capillaries of the preform. For slow infiltration velocities, a fingering of the infiltration front can be observed with large pore channels being filled first. Higher infiltration velocities lead to a more homogeneous infiltration front.[29] During this phase, the hydrodynamic forces lead to a pressure drop across the preform height. For constant pressure experiments, as those that use gas pressure infiltration, the infiltration speed is dependent on the pressure applied, whereas for squeeze-casting setups the infiltration speed

is given by the plunger speed with the pressure-builtup as the answer of the system. Until the whole thickness has been infiltrated, pressure will increase linearly with infiltration time. The increase in pressure will be steeper for increased fluid velocities as has been shown by Long.[33] Using Darcy's law, the pressure drop ΔP of a fluid flow $\dot{V}$ of viscosity η through a porous sample with a thickness L, cross section A and a permeability D can be calculated as

$$\Delta P = \frac{\dot{V} L \eta}{A D} \tag{2}$$

A high flow resistance can lead to a high pressure drop which in turn can result in a compression or breaking of the sample. A high permeability is desirable because of the reduction in hydrodynamic pressure but on the other hand a high porosity will result in very low strengths of the porous body. A balance between flow resistance and strength has to be found. Fig. 3 shows the calculated pressure drops for several fluid velocities across a sample of a thickness of 10 mm depending on the permeability. Viscosity of the aluminium melt has been assumed[30] as 1.15 mPa s which is very close to that of water. The plotted velocity of 0.0283 m/s corresponds to the aluminium velocity in the squeeze casting experiments conducted for this report for a preform of 60% porosity. It is obvious that for high infiltration velocities as those that occur during pressure die-casting (in the order of m/s), only preforms with a very high permeability will be able to withstand the infiltration pressure. It is important to tailor the porosity to achieve a high permeability with at least a sufficient strength level. Porous ceramics made by sintering of coarse powders have been reported[20] with permeabilities in the order of 10^{-15}–10^{-14} m^2 and it is obvious that they will be unsuitable for infiltrations with high fluid velocities. Fluid velocities cannot be too low either or a solidification of else the melt will occur before the preform has been fully infiltrated, unless the whole setup is above the solidification temperature which will lead to other problems such as unwanted chemical reactions, expensive tool materials and sealing difficulties for squeeze-casting processes.

This discussion is strictly valid only for ideal, static conditions with laminar flow, but it gives a good estimate of what could be expected and which preform amid process parameters have the greatest influence. Even for high melt velocities the flow is expected to be mostly laminar and completely laminar for the low flow rates used in squeeze casting. Fig. 4 shows the Reynolds number Re

$$Re = \frac{\rho u d}{\eta} \tag{3}$$

of a melt of density ρ as a function of the pore diameter d for several melt velocities u. For a flow through a circular pipe the transition from laminar to turbulent flow is expected at $Re > 2300$. This transition occurs at smaller values for rough surfaces and non-ideal pipe shapes with varying diameters. Since the pore structure in the preforms is far from ideal it will be considerably lower than 2300 but even with that, turbulent flow is only expected for pressure casting infiltration with melt velocities in the order of several meters per second.

2.2.3. Compression

After the whole preform has been penetrated in squeeze casting, a steep increase in pressure occurs. The point of inflection of the pressure/time-curve is called the penetrating-through pressure. A further increase in pressure will lead to further compression and filling of micropores in the matrix that have not been filled by the previous fluid flow, and trapped air bubbles will be compressed. In this stage of the process, the infiltration

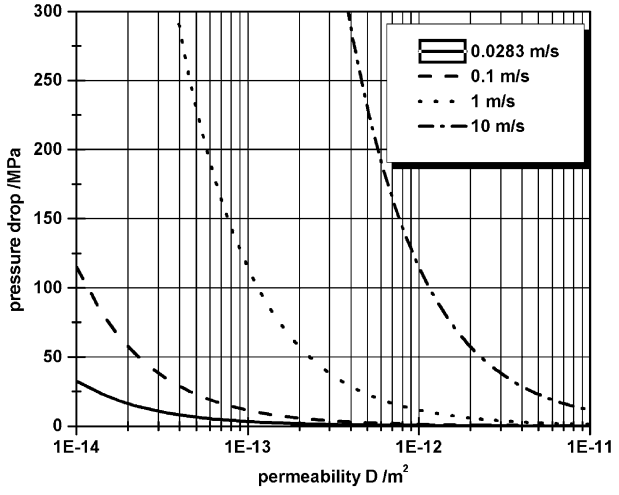

Fig. 3. Pressure drop for Darcian flow depending on permeability and fluid velocity for a body of 10 mm thickness.

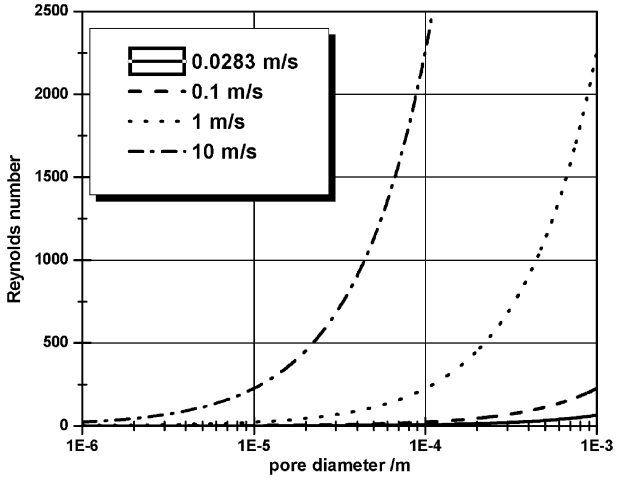

Fig. 4. Reynolds number of a capillary melt flow depending on pore diameter and fluid velocity.

will again be dominated by the capillary force discussed above as little material has to flow to fill the low-volume pores of submicron diameter and only a few micrometres of length. It is important to solidify under high pressure to feed the solidification shrinkage of the melt to avoid delamination and cavitation. Pressures in the order of 100 MPa are typical for squeeze casting like experiments whereas gas infiltration setups usually work in the range of 10–30 MPa.

3. Experimental

3.1. Preform preparation

Aqueous alumina suspensions were prepared using Alcoa CT3000SG alumina powder with a medium diameter of 0.7 μm. Zschimmer & Schwarz Dolapix CE 64 was added as a dispersant. The powder was dispersed and de-agglomerated using ultrasound, then degassed under vacuum for 1 h and homogenised on rollers for 24 h. Varying amounts of pyrolysable pore forming agents (PFAs) and deionised water were added to this master suspension with the same processing steps as above. Amounts were chosen so that a range of porosities between 50% and 67% could be obtained to study the influence of alumina content on the composite properties which will be published in a future study.

The PFAs used in this work were commercial potato starch (Kartoffelmehl, Toffena) and maize starch (Hylon VII, National Starch). Both were of equiaxed and almost spherical shape with the size distributions given in Fig. 5. They were measured using a Sympatec Helos laser diffraction analyser. It is important to note that the starch particles swell when immersed in water. The size distribution of the PFAs corresponds very well with the pore size distribution in the sintered body. Pores in the ceramic are slightly smaller because of the sintering shrinkage. To study the effects of starch swelling and shrinkage a few samples were prepared for comparison with PMMA beads of a size distribution very similar to that of the potato starch, but they show no swelling and shrinkage.

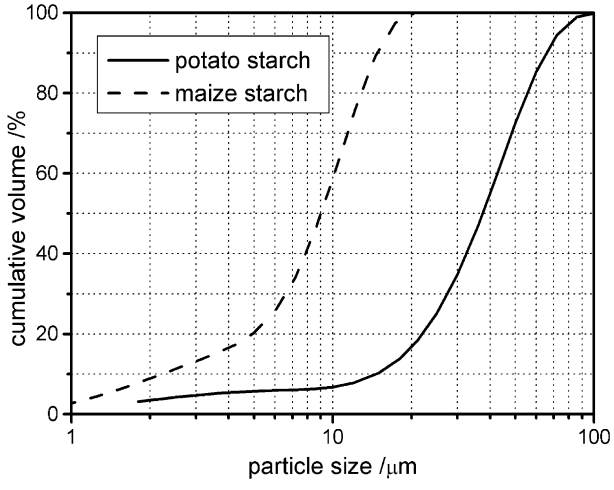

Fig. 5. Particle size distributions of maize and potato starch pore forming agents.

Shaping was done using a laboratory pressure filtration apparatus with a filtration pressure of 1 MPa using rectangular moulds of 55×50 mm and cylindrical ones of 90 and 60 mm diameter. Samples were dried at 20 °C and 90% humidity for 24 h and then at 80 °C for 48 h. The starch was burned out at 750 °C with a 30 °C/h heating rate under air flow. These green bodies were then sintered at 1300 and 1550 °C in air to vary the microstructure of the cell walls. Lower sintering temperatures resulted in partly sintered walls containing submicrometer porosity, whereas high sintering temperatures lead to almost completely dense struts. Porosities were varied between 50% and 67%. In all cases the porosity obtained was almost completely open with about 0.5–1% closed pores as measured by the water immersion method.

3.2. Permeability measurements

Permeability measurements were performed using sintered disks of 47 mm diameter and 7 mm thickness in a pressure nutsche setup. They were immersed in water under vacuum for at least 2 h to completely fill their pores. Then they were mounted in the nutsche and the pressure chamber filled with water. By applying precisely controlled gas pressure, water was driven through the preform and the corresponding mass flow was measured. The permeability was then calculated using Eq. (2).

3.3. Metal infiltration

The rectangular preforms were squeeze infiltrated with a technical AlSi-alloy (AlSi12). This alloy is near eutectic with an eutectic temperature of 577 °C. Before infiltration, the preforms were heated up to 800 °C in a furnace to prevent premature melt solidification. The graphite coated die (65×46×35 mm) was preheated to 450 °C in a Fontune TP400 laboratory platen press. The alloy was superheated to 800 °C. During composite casting the following steps took place sequentially: placing the heated preformn into the die, pouring the melt into the cavity, placing the upper punch, closing the hydraulic press with a plunger speed of 17 mm/s amid a maximum pressure of 100 MPa. This was maintained until the complete solidification of the alloy was achieved. After solidification, the composite was ejected. To obtain the average melt velocity in the preform the plunger speed has to be divided by the preform porosity.

4. Experimental results

4.1. Preform inicrostructure

Preform SEM images were taken of surfaces cut with a diamond saw without additional polishing in a Leica Stereoscan 440. The effect of the variation of the sintering temperature can be seen in Fig. 6A and B. Preforms sintered at 1300 °C show a microporous wall with small grains sintered together at the contact points whereas those sintered at 1550 °C are dense with pronounced grain growth.

Fig. 7A shows the microstructure of a preform based on maize starch. The microstructure is homogeneous and fine, with walls of less than 10 μm thickness. The necks between pores at the contact points are in the 5 μm range are not very pronounced. In some cases no clear distinction between individually replicated pores is possible, creating a very uniform overall pore diameter with full percolation. This is very different from the potato starch-based microstructure shown in Fig. 7B. The microstructure is less homogeneous with all pores distinctly based on individual starch particles which are all interconnected. Necks leading to a percolation are clearly visible and frequent, ranging up to approximately 20 μm diameter. The walls are also not as homogeneously formed as with the maize starch-based samples with thicknesses of up to 30 μm. The overall porosities in both preforms was the same with 63%. Both microstructures show globular ceramic agglomerates in many of the pores. These were also visible on fracture surfaces of the green body. The same structures can be seen in other works on starch-based porous ceramics[21–23] that used a wet shaping process whereas they could not be observed in dry pressed samples. To the authors' knowledge this effect has not been discussed in literature before. Fig. 8 shows the microstructure of a preform made with PMMA beads. Comparing that with the potato starch shows that the number of interconnects between the pores is much lower and the existing necks are smaller. In many cases pores are very close to each other with the wall between them intact whereas pores made from potato starch connect when they are at similar distances. None of the

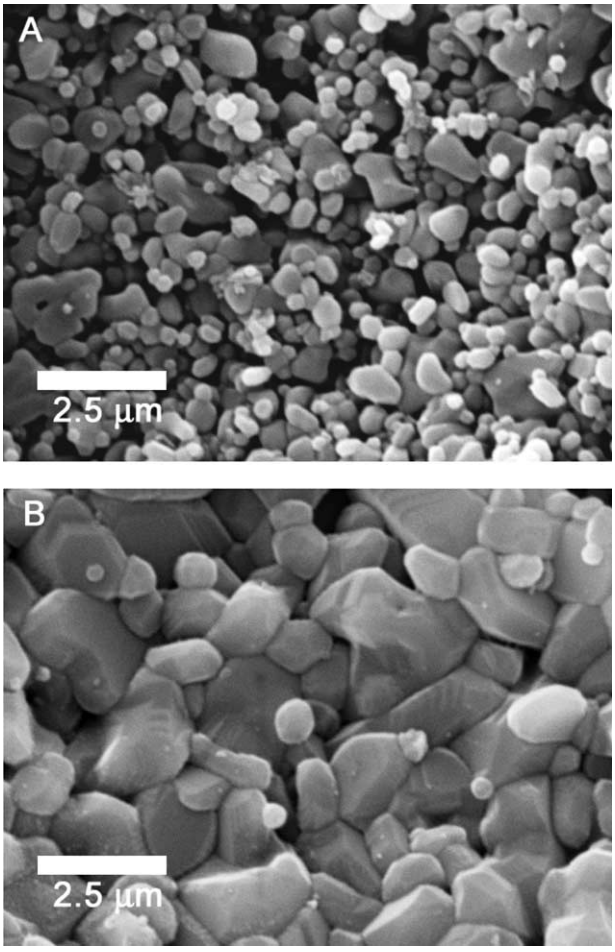

Fig. 6. Pore wall microstructure: (A) sintering temperature of 1300 °C, small grains with a microporous structure; (B) sintering temperature of 1550 °C, large grains with a dense structure.

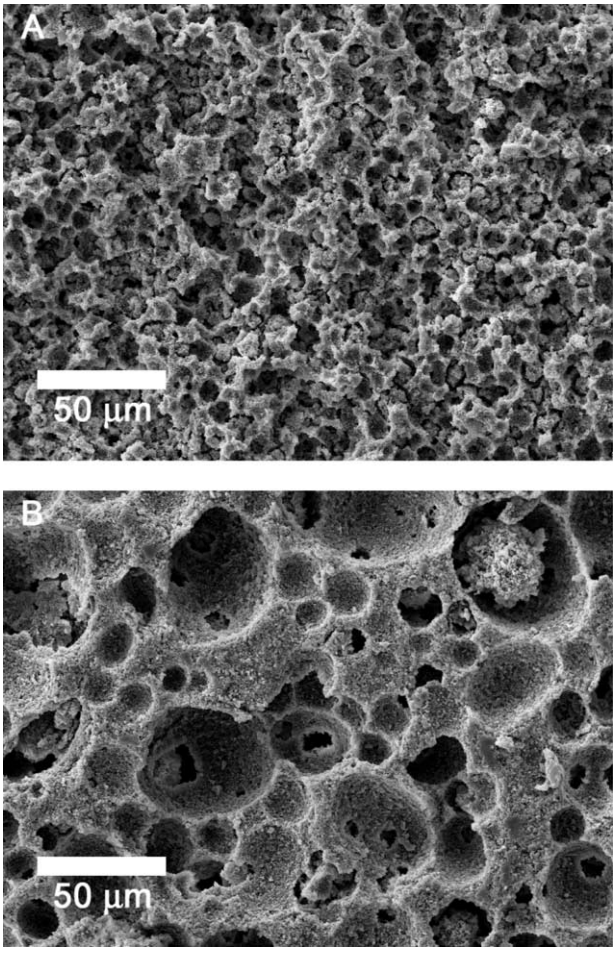

Fig. 7. Preform microstructure: (A) maize starch-based, 63% porous, sintered at 1300 °C; (B) potato starch-based, 63% porous, sintered at 1300 °C.

globular agglomerates are present and cracks are visible around the pores.

It is obvious that the globular clusters are an effect of drying. Starch particles take on water and swell when suspended in it. During drying the particles shrink more than the surrounding ceramic matrix and some powder sticks onto them, sintering together during the sinter stage. This opens walls between neighbouring starch particles which were not connected before, and enlarges existing necks. With PMMA beads the effect is different, the particles are rigid and the drying matrix shrinks onto them, leading to cracks in the matrix around the particles which do not heal during sintering.

4.2. Permeability

Fig. 9 shows the permeabilities for potato and maize starch-based preforms of 58% porosity for a range of pressures. The average value for maize starch was 9.7×10^{-14} m^2, that for potato starch 6.3×0^{-13}m^2 independent of pressure. This shows a strong influence of the pore structure on the permeability so that fewer, larger pores offer less flow resistance than many smaller ones. It also indicates that microporous pore walls will offer only a negligible contribution to fluid flow.

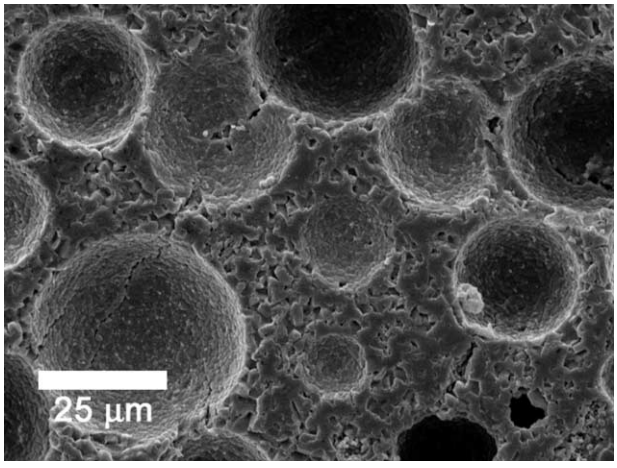

Fig. 8. Preform microstructure, PMMA-based, 55% porous, sintered at 1550 °C.

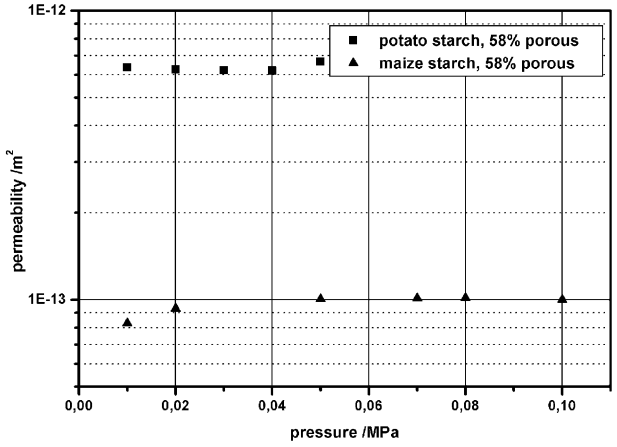

Fig. 9. Permeabilities for maize and potato starch-based preforms, 58% porous sintered at 1300 °C.

4.3. Preform bending strength

Preform four-point bending strength of the preforms was measured with a universal testing machine UTS 10T. Sample geometry was 48×8×3 mm. Fig. 10 shows the Weibull diagram and Table 1 gives the parameters for several preform compositions. A strong dependance on porosity is obvious while the microstructure had a minor influence as the results show for two compositions with 57% and 58% porosity. Sintering at 1300 °C was enough to obtain samples of adequate strength for easy handling even for the composition with the highest PFA content.

4.4. Composite microstructure

Fig. 11A and B show micrographs of composites taken by optical microscopy. The dark grey phase represent alumina, the bright one aluminium and the medium grey stripes in the aluminium eutectic silicon precipitations. The whole macroporosity was infiltrated with no visible delamination and cavitation of the aluminium. The globular alumina agglomerates in the pores are present in most of the pores. Their packing was loose and contained microporosity even when

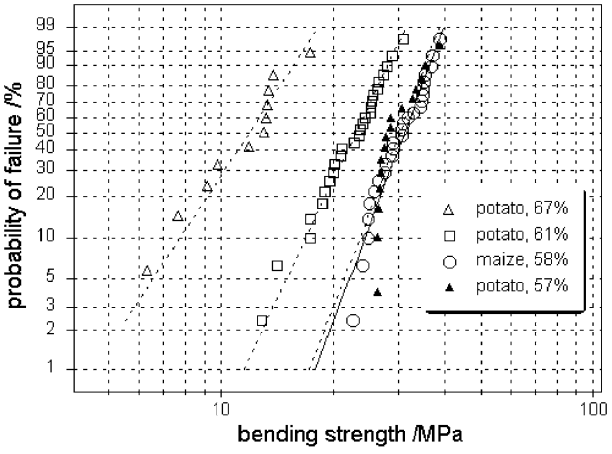

Fig. 10. Weibull diagram of preform four-point bending strength.

Table 1
Preform four-point bending strength

Starch type	Porosity (%)	Strut microstructure	σ_0 (MPa)	m
Potato	67	Porous	12.9	4.4
Potato	61	Porous	24.4	6.1
Maize	58	Porous	32.6	7.7
Potato	57	Dense	31.6	7.6

sintered at 1550 °C, which was fully infiltrated by the aluminium. The maize starch-based composite shows some dense alumina agglomerates of approximately 25 μm diameter which were riot destroyed during processing but otherwise the microstructure is relatively homogeneous. The SEM magnification in Fig. 11B shows a microporous pore wall section which has been almost completely infiltrated with approximately 1% porosity visible as black pores. Silicon precipitations have occured in the cell walls as well.

5. Discussion

The obtained composite microstructures were in accordance with the predictions discussed in Section 2.2. The four-point bending strength of the performs was greater than 10 MPa in all cases with the compressive strength expected to be even higher than that. This was greater than the threshold pressure predicted according to capillary law as shown in Fig. 2 of approximately 0.2 MPa for 5 pm pores as expected for the maize starch-based preforms. Dynamic stresses during the melt flow phase for the worst permeability of approximately 10^{-13} m^2 were estimated to be less than 5 MPa whereas the corresponding preforms based on maize starch had a four-point bending strength of 32 MPa. For more porous and thus more permeable preforms the stresses were expected to be much lower and below the strength in any case. After full penetration of the preform thickness a steep increase in pressure was expected with compression and filling of micropores that were not infiltrated with the lower dynamic pressures. For 100 MPa, capillary law predicts infiltration of pores of 20 nm diameter so the microporous walls should have been fully penetrated, as found by SEM investigations. A small remaining porosity was present, some of which may be the closed porosity of the preform as determined by the water immersion method. Other small pores might have been closed off by premature melt solidification or contain highly compressed air caught in the matrix. The influence of this small remaining porosity on mechanical properties is estimated to be negligible or at least much smaller than a comparable amount of porosity would have in monolithic ceramics without a ductile metal phase.

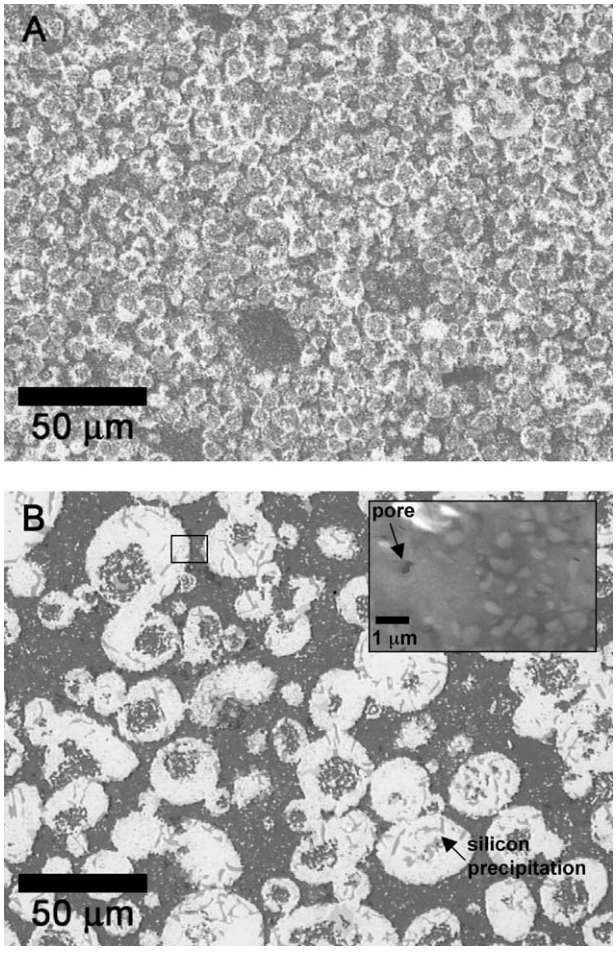

Fig. 11. Composite microstructure: (A) maize starch-based, 37% ceramic content; (B) potato starch-based, 33% ceramic content with magnified microporous pore wall section from SEM studies.

The influence of the globular starch agglomerates within the macropores has to be investigated further. SEM images suggest that the effect on permeability is beneficial because the number of interconnects between pores is much higher than with non-shrinking PFAs such as the PMMA beads. The neck diameter which is the limiting factor for fluid flow is also enlarged. The agglomerates themselves represent an obstacle for the melt flow but especially the increased number of interconnects will more than compensate for that. The structures themselves were fully infiltrated by the metal melt. Especially for the maize starch-based composites, this lead to a very homogeneous microstructure with a permeability that can only be obtained by the sintering of very coarse powders for processing routes without PFAs. Such a microstructure with fine ceramic grains might show very good tribological properties which are currently under investigation. The influence of microstructure and ceramic content on mechanical and thermal properties will be published elsewhere.

6. Summary

Fully interpenetrating alumina–aluminium composites were obtained by infiltration of molten aluminium into porous ceramnic preforms by a direct squeeze-casting process. By varying the content and size of spherical pore forming agents the macropore-structure was determined. Microporosity in the pore walls was influenced by a variation of the sintering temperature. Measurements of permeability and preform strength

were compared to theoretical considerations based on capillary law and Darcian flow. The experimental observations on adequacy of strength and minimium pore diameter infiltrated matched the expectations of the calculations. The pressure of 100 MPa used in the squeeze-casting process was sufficient to infiltrate even the microporous walls of the preforms sintered at low temperatures so that an interpenetration was achieved both on the macro- and microscale. The influence of this microstructure on composite properties is under investigation.

Acknowledgements

This work was conducted within the project "Interpenetrierte Metall-Keramik-Verbundwerkstoffe (Preform-MMC) für thermisch und tribologisch hochbeanspruchte Leichbauteile" funded by the Landesstiftung Baden-Württemberg, Germany.

References

1. Lloyd, D. J., Particle reinforced aluminium and magnesium matrix composites. *International Materials Reviews*, 1994, **39**, 1–23.
2. Clyne, T. and Withers, P., *An Introduction to Metal Matrix Composites,* 1st edn. Cambridge University Press, Cambridge, 1993.
3. Clyne, T., Metal matrix composites: matrices and processing, In. *Encyclopaedia of Materials: Science and Technology*. Pergamon, 2001, (Ch. 3.7.12).
4. Evans, A., Perspective on the development of high-toughness ceramics. *Journal of the American Ceramic Society*, 1990, **73**, 187–206.
5. Flinn, B., Lo, C., Zok, F. W. and Evans, A., Fracture resistance characteristics of a metal-toughened ceramic. *Journal of the American Ceramic Society*, 1993, **76**, 369–375.
6. Clarke, D. R., Interpenetrating phase composites. *Journal of the American Ceramic Society*, 1992, **75**, 739–759.
7. Knechtel, M., Prielipp, H., Müllejans, H., Claussen, N. and Rödel, J., Mechanical properties of Al/Al_2O_3 and Cu/Al_2O_3 composites with interpenetrating networks. *Scripta Metallurgica et Materialia*, 1994, **31**, 1085–1090.
8. Fan, Z., Tsakiropoulos, P. and Midownik, A., Prediction of Young 's modulus of particulate two phase composites. *Materials Science and Technology*, 1992, **8**, 922–929.
9. Nardone, V., Strife, J. and Prewo, K., Microstructurally toughened particulate-reinforced aluminium matrix composites. *Metallurgical Transactions A*, 1991, **22A**, 171–182.
10. Evans, A. and McMeeking, R., On the toughening of ceramics by strong reinforcements. *Acta Metallurgical*, 1986, **34**, 2435–2441.
11. Sigl, L., Mataga, P., Dalgleish, B., McMeeking, R. and Evans, A., On the toughness of brittle materials reinforced with a ductile phase. *Acta Metall*, 1988, **36**, 945–953.
12. Thouless, M., A re-examination of the analysis of toughening in brittle matrix composites. *Acta Metallurgical*, 1989, **37**, 2297–2304.
13. Prielipp, H., Knechtel, M., Claussen, N., Streiffer, S., Müllejans, H., Rühle, M. and Rödel, J., Strength and fracture toughness of aluminum/alumina composites with interpenetrating networks. *Material Science and Engineering*, 1995, **A197**, 19–30.
14. Skirl, S., Hoffman, M., Bowman, K., Wiederhorn, S. and Rödel, J., Thermal expansion behavior and macrostrain of Al_2O_3/Al composites with interpenetrating networks. *Acta Materialica*, 1998, **46**, 2493–2499.
15. Lange, F. F., Velamakanni, B. and Evans, A., Method for processing metal-reinforced ceramic composites. *Journal of the Ceramic Society*, 1990, **73**, 388–393.
16. Cichocki, F. C. Jr., Trumble, K. and Rödel, J., Tailored porosity gradients via colloidal infiltration of compression-molded sponges. *Journal of the American Ceramic Society*, 1998, **81**, 1661–1664.
17. Peng, H., Fan, Z. and Evans, J., Novel MMC microstructure prepared by melt infiltration of reticulate ceramic preforms. *Materials Science and Technology*, 2000, **16**, 903–907.
18. Xu, Y. and Chung, D., Low-volume-fraction particulate preforms for making metal–matrix composites by liquid metal infiltration. *Journal of Materials Science*, 1998, **33**, 4707–4709.
19. Corbin, S. F., Lee, J. and Qiao, X., Influence of green formulation and pyrolyzable particulates on the porous microstructure and sintering characterisitcs of tape cast ceramics. *Journal of the American Ceramic Society*, 2001, **84**, 41–47.
20. Dröschel, M., *Grundlegende Untersuchungen zur Eignung poröser Keramiken als Verdampferbauteile*. Dissertation Institut für Keramik im Maschinenbau Universität Karlsruhe, 1998.
21. Corbin, S. F. and Apte, P. S., Engineered porosity via tape casting, lamination and the percolation of pyrolyzable particulates. *Journal of the American Ceramic Society*, 1999, **82**, 1693–1701.
22. Davis, J., Kristoffersson, A., Carlström, E. and Clegg, W., Fabrication and crack deflection in ceramic laminates with porous interlayers. *Journal of the American Ceramic Society*, 2000, **83**, 2369–2374.
23. Galassi, C., Roncari, E., Capiani, C., Fabbri, G., Piancastelli, A., Peselli, M. and Silvano, F., Processing of porous PZT materials for underwater acoustics. *Ferroelectrics*, 2002, **268**, 47–52.
24. Lopes, R. and Segadaes, A., Microstructure, permaebility and mechanical behaviour of ceramic foams. *Materials Science and Engineering*, 1996, **209**, 149–155.
25. Dröschel, M., Hoffmann, M. J., Oberacker, R., Both, H. V., Schaller, W., Yang, Y. Y. and Munz, D., SiC-ceramics with tailored porosity gradients for combustion chambers. *Engineering Ceramics: Multifunctional Properties—New Perspectives*, 2000, **175–176**, 149–162.
26. Mattern, A., Oberacker, R., Hoffmann, M., Multi-phase ceramics by computer-controlled pressure filtration. *Journal of the European Ceramic Society*, doi: 10.1016/j.eurceramsoc.2003.10.037.
27. Aghajanian, M., Rocazella, M., Burke, J. and Keck, S., The fabrication of metal matrix composites by a pressureless infiltration technique. *Journal of Materials Science*, 1991, **26**, 447–454.
28. Srinivasa Rao, B. and Jayaram, V., New technique for pressureless infiltration of Al alloys into $A1_2O_3$ preforms. *J. Mater. Res.*, 2001, **16**, 2906–2912.
29. Garcia-Cordovilla, C., Louis, E. and Narciso, J., Overview no. 134—pressure infiltration of packed ceramic particulates by liquid metals. *Acta Materialia*, 1999, **47**, 4461–4479.
30. Kaufmann, H. and Schulz, P., Filling of continuous fiber preforms during isothermal gas pressure infiltration. *Aluminium*, 2000, **76**, 75–79.
31. Coupard, D., Goni, J. and Sylvain, J., Fabrication amid squeeze casting infiltration of graphite/alumina preforms. *Journal of Materials Science*, 1999, **34**, 5307–5313.
32. Kaufmann, H., Auer-Knöbel, R. and Degischer, H., Elevated temperature properties of short-fiber reinforced AlSi9Cu3 produced by pressure die-casting. *Zeitschrift für Metallkunde*, 1994, **85**, 241–248.

33. Long, S., Beffort, O., Moret, G. and Thevoz, P., Processing of Al-based MMCs by indirect squeeze infiltration of ceramic preforms on a shot-control high pressure die casting machine. *Aluminium*, 2000, **76**, 82–89.
34. Kalazhokov, K. K., Kalazhokov, Z. K. and Khokonov, K. B., Surface tension of pure aluminum melt. *Technical Physics*, 2003, **48**, 141–142.
35. Li, J.-G., Wetting of ceramic materials by liquid silicon, aluminium and metallic melts containing titanium and other reactive elements: a review. *Ceramics International*, 1994, **20**, 391–412.